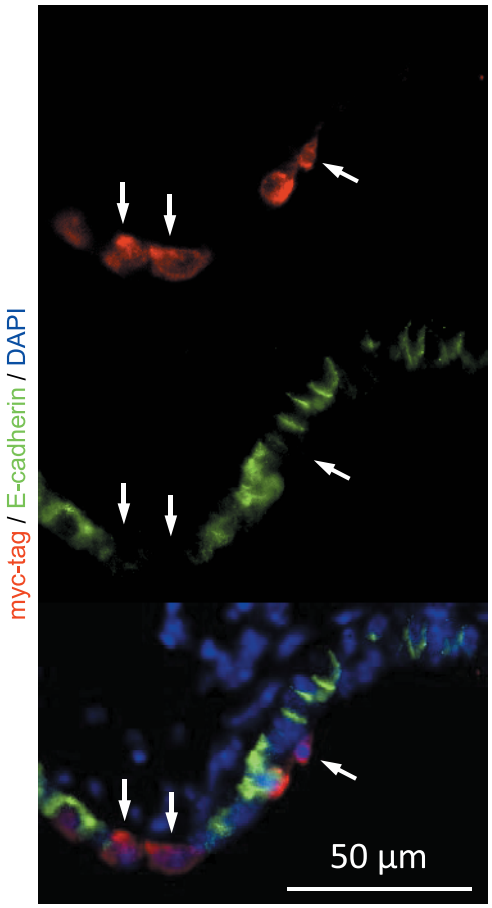

Figure W1. Analysis of subcellular distribution of endogenous E-cadherin in conducting airway cells after dn E-cadherin expression. Representative dual immunofluorescence staining of lung sections from induced DTR mice for myc tag (red) and E-cadherin (green). Images are representative of $n = 3$ separate mice per treatment group. Arrows indicate myc tag–expressing cells that are negative for E-cadherin. Nuclei were counterstained with DAPI (blue).

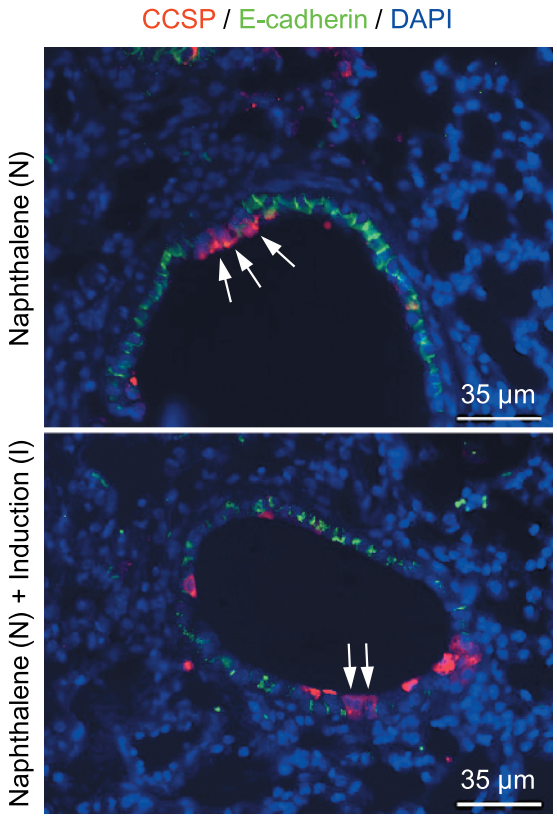

Figure W2. Analysis of CCSP and E-cadherin expression in conducting airways after naphthalene treatment. Dual immunofluorescence staining of lung sections for CCSP (red) and E-cadherin (green). Images are representative of $n = 3$ separate mice per treatment group. Five-week-old mice were treated as indicated. Mice were recovered following 2 days from naphthalene exposure. Arrows indicate naphthalene-resistant Clara cells.

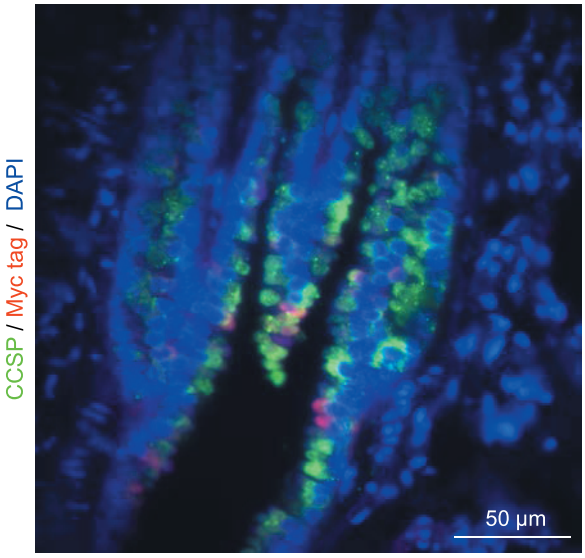

Figure W3. Analysis of the transgene expression in induced hyperplastic lesions. Double immunofluorescence staining of a representative lung section from an induced mouse for the indicated markers shows that only minority of the hyperplastic cells express the transgene.

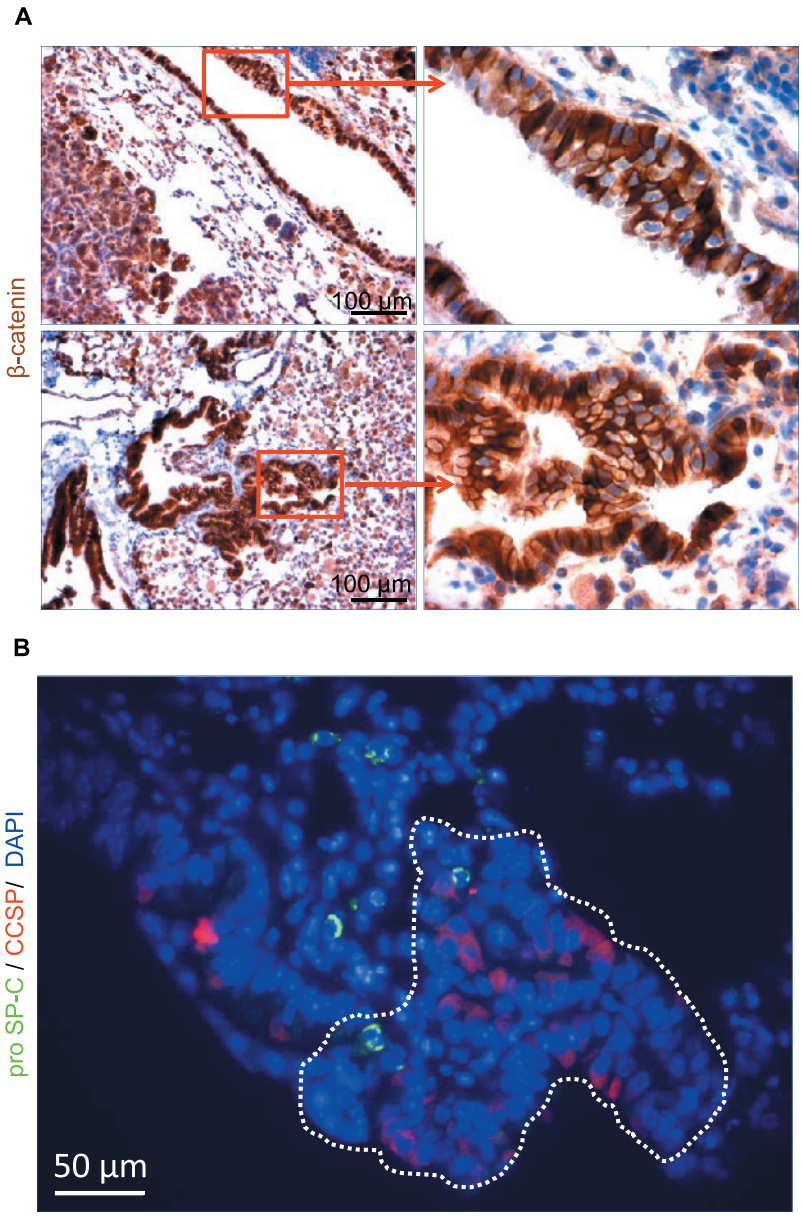

Figure W4. (A) β-Catenin immunohistochemistry and analysis of abundance of alveolar type II cells in the hyperplasia. (A) Paraffin-embedded lung sections from induced DTR mice stained for β-catenin (brown). Right panel pictures are the high magnification of the insets. Hematoxylin (blue) was used as a counterstain. (B) Double immunofluorescence staining of a representative hyperplastic lesion for CCSP (red) and pro SpC (green) shows that most of the cells in the hyperplasia are negative for pro SpC. Nuclei were counter-stained with DAPI (blue). Dotted lines outline the hyperplastic area.

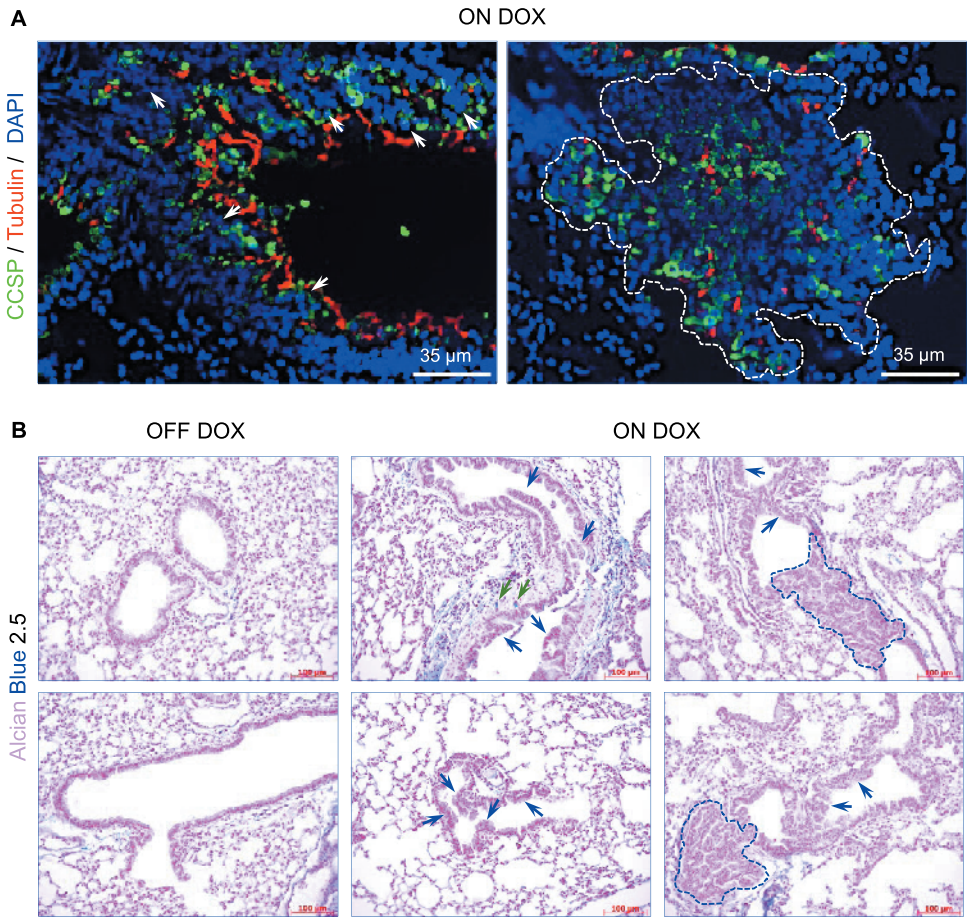

Figure W5. Analysis of abundance of ciliated and goblet cells in induced bronchiolar hyperplasia. (A) Double immunofluorescence staining of lung sections from induced mice for indicated markers. Nuclei were counterstained with DAPI (blue). White arrows and the marked region show early and progressive bronchiolar hyperplasia, respectively. (B) Alcian Blue 2.5 staining of lung sections from control (OFF DOX) and induced (ON DOX) mice. Green arrows show Alcian Blue–positive goblet cells. Blue arrows and the marked regions show early and progressive bronchiolar hyperplasias, respectively.

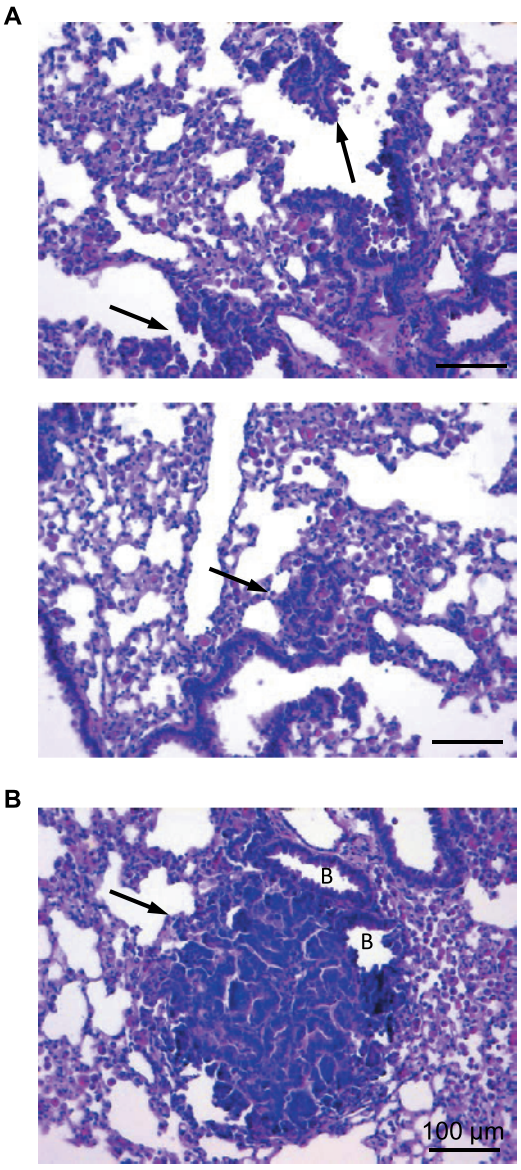

Figure W6. Early lung tumors in induced DTR mice resemble the papillary hyperplastic lesions and are associated with conducting airways. (A) Histologic analysis through H&E staining of lungs from DOX-treated DTR mice showing the epithelial hyperplasia (arrows). (B) H&E staining of a lung section from a 7-month DOX-treated mouse shows a budding lung tumor (arrow) from a bronchiole.

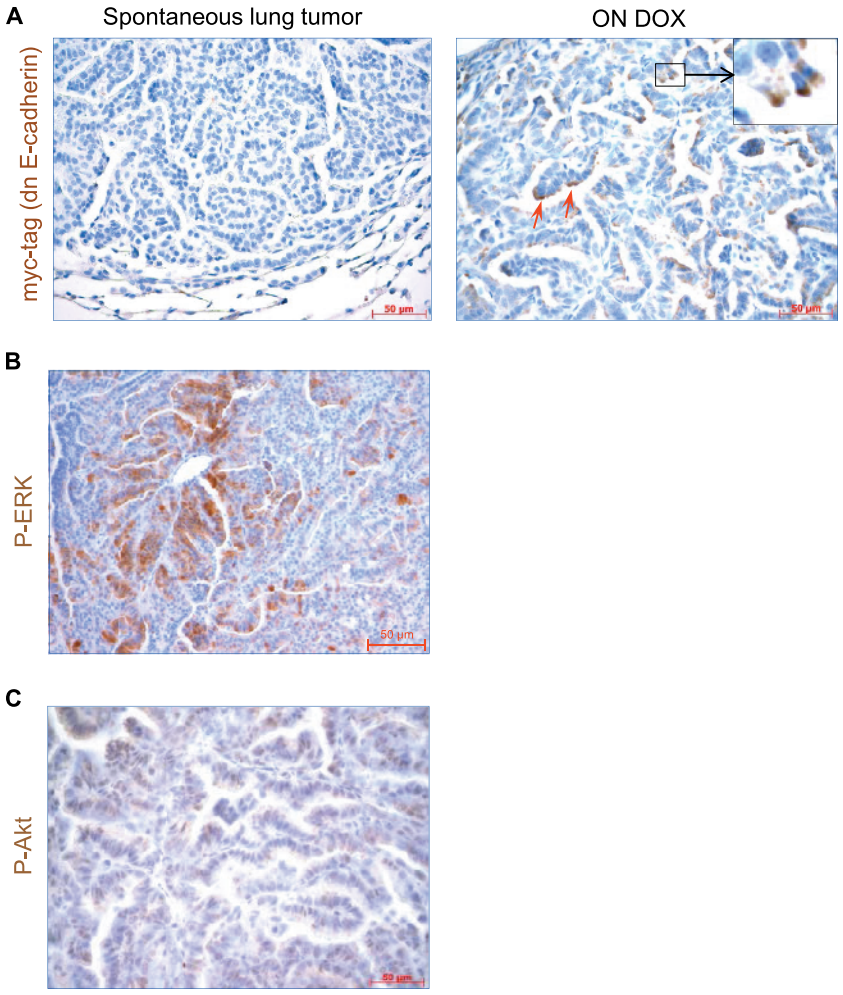

Figure W7. Analysis of transgene, phospho-ERK, and phospho-Akt expression in induced lung tumors. (A) To distinguish spontaneous lung tumors from induced tumors, we performed immunohistochemistry for myc tag on lung sections. Red arrows show myc tag–expressing rare tumor cells in an induced lung tumor. Note the absence of myc tag staining in the spontaneous lung tumor. High-magnification image represents the region shown in the inset. Hematoxylin (blue) was used as a counterstain. Immunohistochemistry of lung tumor sections from a 10-month-old mouse for pERK (B) and for pAkt (C). Hematoxylin (blue) was used as a counterstain.

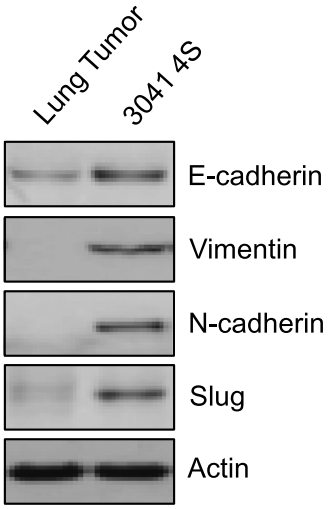

Figure W8. Lack of EMT-associated markers in induced lung tumors. Western blot analysis of a lung tumor from an induced mouse was probed against the indicated markers for evaluation of EMT activation. A mouse NSCLC cell line (3041) transfected with a stabilized form of β-catenin (4S) was used as positive control for the markers.